12

Magnetohydrodynamic instability of the surface metal layer melted by pulsed current

© S.D. Samuilov,[1] I.P. Shcherbakov,[1] Y.N. Bocharov,[2] S.I. Krivosheev,[2] S.G. Magazinov[2]

[1] Ioffe Institute, St. Petersburg, Russia
[2] Peter the Great Saint-Petersburg Polytechnic University, St. Petersburg, Russia
e-mail: sam.mhd@mail.ioffe.ru

Received March 29, 2023
Revised May 16, 2023
Accepted May 22, 2023

It is shown that the results of dispersion of various materials in the mode of pulsed current action correspond to theoretical estimates of the wavelength of MHD instability. The sizes of the obtained metal grain, including refractory ones, correspond to the modes of exposure, and their microstructure corresponds to the conditions of formation. Modeling in the Comsol Multiphysics environment at a qualitative level revealed the influence of the thickness of the surface layer of the current flow on the dynamics of the formation and separation of liquid metal droplets. It is shown that one of the operating factors that create and increase instabilities is the heterogeneity of the distribution of Lorentz forces in the current supply zone.

Keywords: electric explosion, surface effect, grain (micro-ingots), numerical simulation.

DOI: 10.61011/TP.2023.08.57273.61-23

Introduction

The study of the mechanisms of conductors destruction by electric current is a fundamental scientific problem [1] and at the same time, these studies provide a number of applied results that can be used in engineering and technology. In particular, the destruction product — metal granules (micro-ingots) [2] — can find application in promising, rapidly developing additive technologies [3,4], powder metallurgy technologies [5], as well as for the manufacture of filters, catalysts, etc. etc. The paper [1] analyzes the current state of studies in this area and provides an extensive bibliography. In particular, the mode of ultra-fast electric explosion is considered, when the electric current does not have time to penetrate deep into the conductor, and its destruction begins with the destruction of the surface layer — skin mode. These experiments use thin wires that are completely dispersed during the process. In this paper, another variant of the implementation of this physical phenomenon is investigated. Sufficiently thick and strong metal rods are used as the test sample, and even at a very high electric current density on the surface of the conductor, sufficient to melt a thin surface layer, the stability of the conductor as a whole is maintained. In this mode, there is a solid cold rod inside the conductor, and magnetohydrodynamic (MHD) instability destroys the surface layer only of the conductor, due to the skin effect, and this opens up the possibility of studying not only the products of destruction-metal droplets, which, when cooling and crystallizing, form granules, but also traces of instability on the surface of the rod.

1. Problem formulation

This paper considers the case when the energy introduced into the surface layer of a conductor is sufficient to melt a thin layer of material on its surface, but is certainly insufficient to evaporate the material. The sample dimensions and process parameters are selected in such a way as to avoid destruction of the conductor as a whole. To do this, the elastic forces of the cold solid rod shall be sufficient to resist the development of helical instability of the solid conductor. The corresponding criteria were formulated and experimentally confirmed in papers [6,7], the corresponding formulas are given below. In addition to considering the stability of the conductor as a whole with respect to helical instability, as was done in paper [7], it is necessary to analyze the processes in the liquid molten layer on the surface of the conductor (Fig. 1).

The electric current is passed through the conductor, on the surface of which layer of liquid metal is formed; MHD instability is excited in the layer, the possibility of excitation of which is theoretically substantiated in papers [8,9]. The solid rod prevents the conductor destruction, and the liquid begins to move. In places of constrictions the magnetic pressure is greater than in neighboring places, and the liquid, under the influence of magnetic pressure, moves towards the axis of the conductor, and between the constrictions the liquid moves outward. If the kinetic energy of this liquid, which depends on the rate of instability development and is ultimately determined by the magnitude of the current, exceeds the energy of the surface tension of the liquid required to form the separation

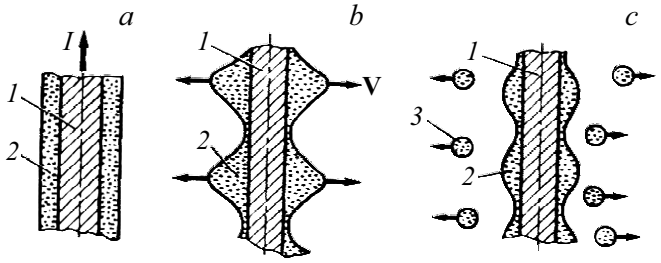

Figure 1. MHD instability of the layer of conducting liquid located on the surface of solid rod when electric current flows through the conductor: *1* — solid rod, *2* — liquid metal that comes into motion as a result of the instability development, *3* — liquid droplets of metal, which, after cooling and crystallization, form granules.

surface, part of the liquid will separate from the rod in the form of droplets. Liquid separation occurs along the knuckle line of the sinusoid. This phenomenon can be used as a method for producing metal granules [10–12], including from refractory reaction metals, and it also leads to the electrodes destruction in a rail accelerator [13]. A similar situation can occur in other devices and processes, in particular during electric welding and melting, and will lead to metal spattering. At the same time, this phenomenon can be used for treatment of parts and samples.

In the experiment, this situation first occurs when studying helical instabilities of solid conductors with a pronounced surface effect, i.e. strongly skinned current [7]. The destruction of the surface layer of the sample was regarded by the authors as a demonstration of the fundamental possibility of achieving uniform evaporation of metal from the surface of the conductor, provided that helical instability does not have time to develop. However, analysis of the surface of the obtained samples revealed traces of instability and showed that it is necessary to consider the stability of the liquid metal layer on the surface of the conductor itself.

2. Results of theoretical studies

In papers [8,9] such a theoretical consideration was carried out under the same assumptions under which the stability of liquid cylinder with current was considered. Formulas [10] were obtained that make it possible to calculate the instability wavelength λ, the minimum current required to separate metal droplets from the rod $I_{\min}$, and the minimum required its transmission time t, the size of the resulting droplets (granules) d_g. The maximum possible current value $I_{\max}$ is determined from the stability condition of the solid rod [7]:

$$\lambda = 140d\left[\frac{\alpha\delta^2}{dI^2}\right]^{1/4}, \tag{1}$$

$$I_{\min} = 10^4\sqrt{\frac{\alpha d^3}{\Delta^2}}, \tag{2}$$

$$I_{\max} = \frac{2\cdot 10^3(d-\delta)^2\sqrt{E_Y}}{l\sqrt{\ln\frac{4l}{\pi(d-\delta)}-1.077}}, \tag{3}$$

$$t = 6\cdot 10^3\sqrt{\frac{\Delta\rho d^3}{I^2}}, \tag{4}$$

$$d_g = 20\left(\frac{\alpha\delta^2 d^3\Delta^4}{I^2}\right)^{1/8}. \tag{5}$$

Here d — workpiece diameter, α — surface tension coefficient of liquid metal, δ — skin layer thickness for current, I — the magnitude of the electric current flowing through the sample (during theoretical considerations the current value is considered constant; in calculations, the amplitude of the current pulse is taken as the current value, which ensures good agreement between the calculations and experiment), Δ — thickness of the molten layer on the surface of the sample, E_Y — modulus of elasticity of the cold material of the sample, l — length of the sample, ρ — density of liquid metal. Formula (1) is presented in the paper [10] on the basis of a theoretical analysis of instability performed in the paper [8], in which the thickness of the molten layer was taken to be equal to the thickness of the layer through which the current flows. Later in the paper [9] a more general case was considered when these values do not coincide. It was established that the wavelength depends not on the thickness of the molten layer, but on the thickness of the layer through which the current flows. Besides, in the paper [6] it is shown that the conductor destruction by current can occur after the end of the current pulse, in the ballistic mode, and accordingly the minimum time of current transmission (4) can be reduced to value approximately equal to the time constant of instability development. Since the liquid metal begins to move in a shorter time, the requirements for the minimum current required to separate the metal from the rod are reduced (2).

3. Analysis of instabilities on surface of thin copper conductors

In the paper [10] we studied copper samples provided by the authors of the paper [7]. In this paper the melting and

Figure 2. Photograph of special copper sample after passing pulsed electric current. Traces of instability in the form of transverse stripes are visible on the surface.

Figure 3. Photograph of copper sample after passing electric current. Amplitude of current pulse is 130 kA.

dispersion of special copper samples (Fig. 2) are carried out by a high-frequency current pulse excited by the discharge of low-inductance capacitor bank with a capacity of $3\,\mu$F with a maximum charging voltage of 50 kV. The frequency of the discharge circuit is 250 kHz, the amplitude of the current pulse is 130 kA, the nature of the discharge is periodic, damped. A copper cylindrical sample with a diameter of $d = l.5$ mm and length of $l = 10$ mm was used as a workpiece. Melting of the copper layer on the surface of the conductor begins at the current pulse amplitude ~ 100 kA. The thickness of the molten layer increases linearly with current amplitude (charging voltage) increasing, and at current amplitude of 130 kA (charging voltage 50 kV) thickness is $\Delta = 40$ mm. Estimated granule size is $d_{gr} = 60$ mm. The thickness of the material layer dispersed during one pulse was determined by weighing the conductor after each current pulse. At a small charging voltage on the battery, the weight of the conductor does not change (the current value is insufficient to melt the surface layer), and starting from a certain voltage the linear increase in the thickness of the dispersed layer begins (which corresponds to linear increase in the thickness of the molten layer), and at maximum charging voltage of 50 kV, the thickness of the dispersed layer is $20\,\mu$m, while the thickness of the molten layer is $40\,\mu$m.

Fig. 3 shows the photograph of sample after passing current pulse through it. It is assumed that the photograph shows formed but not detached droplets of metal. The size of these droplets (granules) was determined using an IZA-2 comparator. 80% of granules have sizes $80 \pm 40\,\mu$m. The estimated size is $60\,\mu$m.

4. Experiments with bulk samples of other metals

In this paper, a more detailed study of this phenomenon is carried out when current flows through samples whose diameter was significantly greater than the depth of penetration of the field into the material. A number of samples from different metals were studied: copper, brass, duralumin, high-alloy stainless steel 12Kh18N10T, which can be considered as a close analogue of heat-resistant nickel alloys. Samples with a diameter of 9 mm were studied using pulsed current generator, which made it possible to create pulsed current with amplitude of up to 660 kA, with a duration of the first halfcycle of the current of $10\,\mu$s. A batch of stainless steel granules ($\sim 100\,g$) was received and tested.

The installation for producing granules consists of a chamber for cooling and collecting granules, in which the test sample is located, connected to a pulse current generator. The amplitude of the current pulse at an almost constant characteristic impedance of the circuit was determined by the level of the charging voltage on the pulse current generator (PCG). Preliminary experiments with samples from various materials showed that the parameters of the current pulse generated by the PCG are insufficient to study the dispersion process of copper samples, on which only traces of the melting process beginning of the surface layer were observed.

It was possible to melt a layer of metal on the surface of the brass samples, and in some areas of the sample the traces of instability in the form of stripes are visible, but these traces are weakly expressed. When studying duralumin samples, melting of the metal layer was achieved at a significantly lower current. The photograph of the sample is presented in Fig. 4, and the experimental parameters are in the text to it. The surface of the sample has pronounced traces of instability, but traces of the initial small-scale instability were already destroyed. Thus, samples made of these metals turned out to be unsuitable for studying instabilities. The study of these materials from the point of view of generating granules did not seem especially relevant, since granules of these materials can be obtained by simpler methods.

Figure 4. Photograph of duralumin sample. Current amplitude 300 kA, halfcycle $10\,\mu$s, attenuation coefficient 0.8, calculated instability wavelength 0.14 mm, and according to the sample image ~ 1 mm.

5. Investigation of high alloy stainless steel samples

More detailed studies were carried out with samples of high-alloy stainless steel 20N18Kh10T, which can be considered as a close analogue of heat-resistant nickel alloys, granules of which are used in granule metallurgy to produce critical parts, while the existing method for their production is complex and very expensive [4,5,14]. In these experiments both instability and the resulting granules were studied. 100 stainless steel samples were processed, some of the granules ($\sim 100\,g$) were collected from the bottom of the chamber. The samples were treated at a maximum current of 660 kA, and three current pulses were applied to each sample with an interval of approximately 1 min. In this case, subsequent current pulses treated the already heated sample.

Analysis of the oscillograms showed that in each discharge the current maintains a typical shape $I(t) = \frac{U_0}{\rho}\sin\left(\frac{2\pi}{T}t\right)\exp\left(-\frac{t}{\tau}\right)$, where U_0 and ρ — charging voltage and characteristic impedance of circuit, T and τ — discharge period and decay time constant. In this case, the resistance introduced into the discharge circuit during the passage of the second and third pulse increases by $2.5\%\rho$, the characteristic impedance of the circuit in these experiments was 0.118 Ω.

Fig. 5 shows a photograph of the sample and the results of its processing. In the photograph we see that the diameter of the sample in its middle part decreased (by 1 mm), vertical stripes are clearly visible. We consider them as traces of instabilities. Some samples were broken by electrodynamic forces when passing current, so the batch of granules contained large fragment-shaped particles, stuck together particles, as well as a small amount of copper particles from the electrodes. The experimental parameters are given in Table 1, and Table 2 shows the size distribution of the resulting granules.

During the experiments for check the electrical resistance of the samples was measured using a four-contact measurement method. The resistivity of the material was calculated, which turned out to be close to the corresponding value for steel 20N18Kh10T, obtained from the literature. A microsection of the cross section of one of the samples was made, before and after spraying the granules. Compared to the initial state, thermally affected zones are clearly visible, hey locate randomly across the cross-section of the electrode and from the surface to a depth of 0.5−0.7 mm. This value, as one would expect, is somewhat less than the calculated thickness of the skin-layer for the energy introduced into the conductor $\delta/2 = 0.9$ mm.

According to the calculation, the minimum current value required to separate metal droplets from the rod is $I_{\min} = 100$ kA, the maximum possible current value is $I_{\max} = 900$ kA. The experiments were carried out by exposing the samples to a pulsed current with an amplitude of $I = 660$ kA and duration of the first halfcycle of 10 μs.

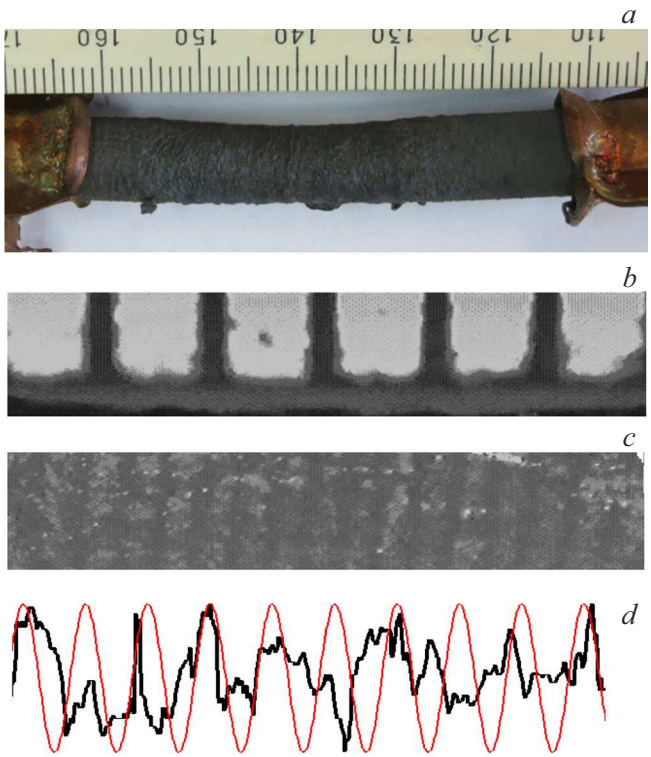

Figure 5. *a* — photograph of sample made of stainless steel 20N18Kh10T after passing three successive current pulses. Enlarged image of the central part of the sample: *b* — ruler area; *c* — central zone of the sample. Transverse stripes are visible - traces of instability. *d* — sample relief and its approximation by a sinusoid.

The instability wavelength λ in the experiment was estimated based on the analysis of the samples surface. The enlarged image of the central part of the sample was scanned according to the degree of the image blackening. The ruler area (Fig. 6, *b*), and the central area of the conductor with clearly visible vertical stripes (Fig. 6, *c*) were scanned. Analysis of the optical profilogram of the obtained image of the central zone (Fig. 6, *d*) showed the applicability of the sinusoidal function for its approximation and determination of the instability wavelength, which was 0.3 mm.

The thickness of the layer of dispersed material varied from experiment to experiment and reached 1 mm, and the formation of initial defects began in the central part of the sample, the development of defects, with increase in the thickness of the dispersed layer, led to the conductor destruction.

6. Stainless steel granules research

Stainless steel granules were analyzed in the laboratories of the All-Russian Institute of Light Alloys (VILS). The size distribution of granules is given in Table 2. It was established that the shapes of granules (dust-like, spherical,

Table 1. Results of experiments on spraying granules of stainless steel 20N18Kh10T

Calculation		Experiment	
Workpiece diameter, d, mm	9	According to calculation	
Workpiece length, l, mm	50	According to calculation	
Electrical resistivity $10^{-7}\Omega$m	7.2	Same during measurement by four-contact method	8–9
Thickness of the skin layer for the inserted into energy conductor, $\delta/2$, mm	0.9	Thickness of heated layer on conductor surface (according to microsection), mm	0.5 –0.7
Melted layer thickness sample surface, Δ, mm	0.1	Not measured	
Minimum current value required for metal droplets separation from rod $I_{\min}$, kA, formula (2)	100	amplitude of electric current I, kA	660
Maximum possible current value $I_{\max}$, kA, formula (3)	900		
Minimum required time of current transmission, t, μs, formula (4)	7	Halfcycle of current pulse, μs	10
According to experimental data		Current attenuation coefficient I_1/I_2	0.8
Instability wavelength λ, mm, formula (1)	0.25	The same for the distance between stripes in the photograph	0.3
Not calculated		Thickness of the material layer dispersed during three current pulse mm	Up to 1
Granule size, μm, formula (5)	200	Fraction with maximum granule content, μm	−250 +180

*Note**: I_1 and I_2 — amplitudes of the first and second half-waves of current.

Table 2. Size distribution of stainless steel granules

Fraction, μm	+400	−400 +350	−350 +300	−300 +250	−250 +180	−180 +140	−140 +100	−100 +70	−70
Content, %	40	13	4	6	12	4	5	4	4

scaly, flakes) have signs of a liquid droplet ingress on the chamber wall. In fact, most of the batch of granules consists of large fragment-shaped particles, as well as sticky particles and flakes. The finely dispersed spherical granules, we are interested in, cover about 20% of the batch. For these granules, the maximum size distribution coincides with the calculated granule size. Fig. 7 shows photograph of the microstructure of spherical granule of the fraction −250 +180, corresponding to the maximum size distribution. The shape of the granules, surface oxidation, microstructure and cooling rate correspond to the conditions of their formation.

The experimental results confirmed the theoretical concepts of MHD instability of layer of conducting liquid located on the surface of the solid rod, and allow us to consider this process as a promising method for producing granules (micro-ingots) of refractory metals. Currently, such granules are in great demand both for traditional granule metallurgy technologies and for the most modern additive technologies [3–5], and the existing production method is complex and very expensive [{]14 }.

The size of the granules is determined by the diameter of the workpiece, the current value and the thickness of the molten layer. The minimum size of granules obtained by this method is several μm, obtaining granules of smaller sizes is impossible due to the increase in the electric current required for dispersion and the insufficient strength of the solid rod compared to the sharply increasing electrodynamic force. There are no fundamental restrictions for obtaining

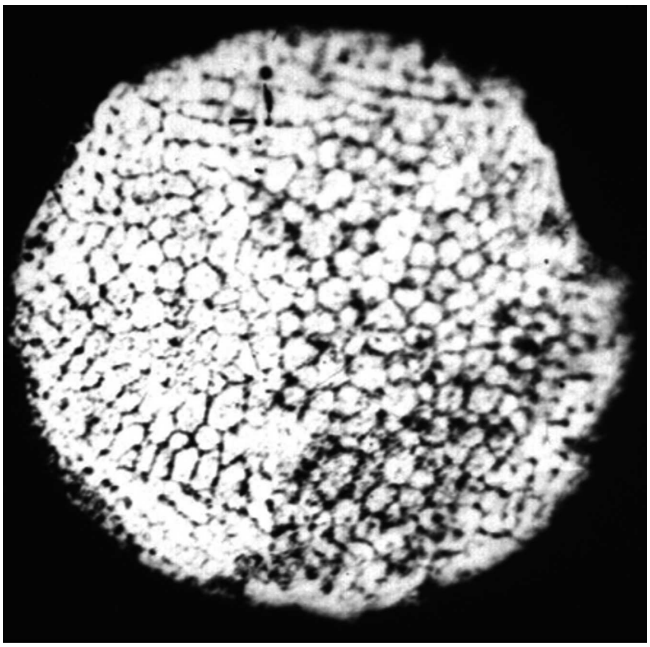

Figure 6. Photograph of granule microstructure of fraction −250 +180. The size of this granule fragment is 180 μm, grain size is 5 μm.

large-sized granules, but the energy required to melt the layer of material increases. A layer of metal can be applied to the rod (including a dielectric one) from the outside; melted by an external heating source, or by passing a high-frequency electric current, which, due to the strong skin effect, flows only in a thin surface layer, or by a short current pulse, which executes both melting and dispersion of the metal. We used current with an amplitude of 660 kA and dispersed the surface layer of the samples with initial diameter of 9 mm. Currently, there are pulsed current generators (PCGs) that generate currents of tens of MA, sufficient to disperse metal from workpieces with diameter of 10 cm or more. At the same time, this dispersion process can be considered as a convenient theoretical and experimental scheme, and the technological process for producing granules may be different. Metallurgists know how to cast metal through thin annular gaps, for example [15], and the methods of supplying current can be different.

7. Analysis of study results

Let us consider the results of this paper in the general picture of the study of the mechanisms of conductors destruction by electric current. With due time, a significant contribution to these studies was made by B.P. Peregud group [6–10]. The mechanisms of conductors destruction identified during those studies were schematically divided by main manifestations and operating factors. 4 zones were distinguished:

1) zone where capillary forces predominate (Rayleigh instability);

2) MHD zone, in which destruction of both solid and liquid conductors occurs;

3) zone of overheating instability, where the conductor destruction is determined by thermal processes;

4) skin mode.

This division was first presented in the dissertation of M.L. Lev, was reported at seminars, but is not presented in the public literature. In modern literature [1] virtually the same approach to the classification of processes is presented, however, 3 zones are distinguished:

1) slow explosion zone (MHD);

2) rapid explosion zone, where thermal processes are decisive;

3) explosion zone of the surface layer of the conductor — skin mode.

In the paper [16] the skin explosion of copper, aluminum, titanium and steel (steel 3 and stainless steel) samples with diameter of $1-3$ mm was studied. The current amplitude was 2.5 MA, and the rise time was 100 ns. As a result of the experiment, the samples were completely dispersed. In the paper [17] copper samples were studied under the same parameters. It was established that the wavelength of MHD instability on the conductor surface was $0.2-0.5$ mm.

Our study relates to the skin explosion zone, and to that part of it where the processes are determined by the development of MHD instability. However, much thicker and stronger conductors were studied, and the input energy was sufficient to melt thin layer on the conductor surface, while there were no conditions for the development of thermal processes, and the current value was insufficient to destroy the conductor as a whole.

We believe that the skin mode of instability development is realized in the case when the thickness of the molten layer on the surface of the conductor is much less than its radius. Then, for typical discharge modes, in which the current through the sample has the form of a strongly damped sinusoid, the minimum size (radius of the conductor) at which the skinned mode of interaction of the discharge current with the conductor is realized, can be determined from the following relation:

$$R_{\min} = \left[\frac{I_0^2}{J_{lb}}\frac{1}{4\pi}\frac{\mu_0}{\rho_s T}\,2\tau\,\frac{1}{\left(\frac{T}{2\pi\tau}\right)^2+4}\left(1-\exp\left(-T/\tau\right)\right)\right]^{0.5} + \left(\frac{\rho_s T}{\mu_0}\right)^{0.5}, \tag{6}$$

where I_0 — current amplitude, ρ_s and J_{lb} — resistivity and critical action integral, $\mu_0 = 4\pi\cdot 10^{-7}$ H/m. Thus, for samples made of high-alloy stainless steel 20N18Kh10T with current amplitude of 660 kA, the minimum radius of the conductor at which the skin mode is formed is $R_{\min} = 3.5$ mm, which supposes the possibility of this

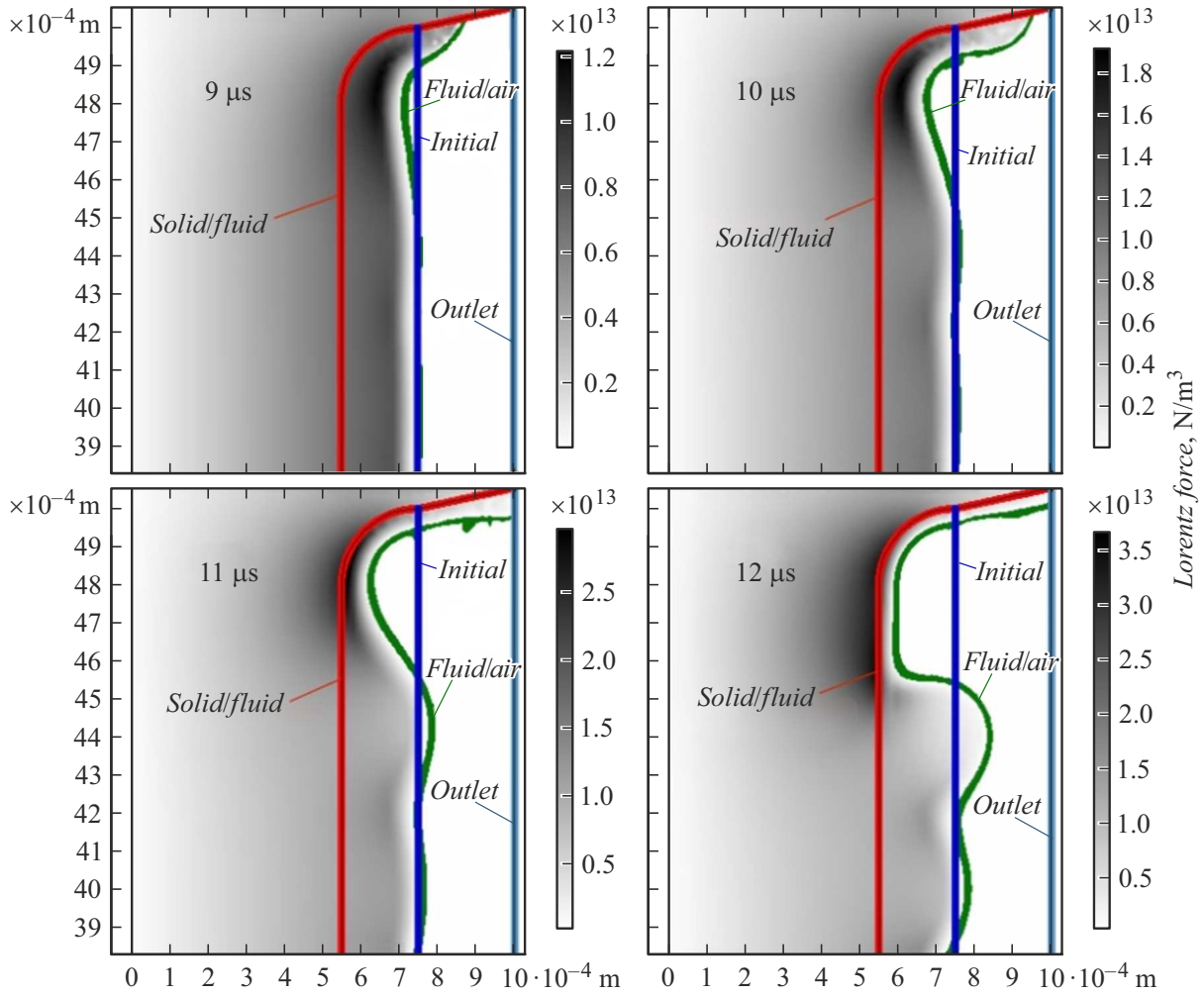

Figure 7. Formation of initial perturbation in cylindrical conductor at the interface with conical current lead with distribution of Lorentz forces at different times when applying voltage linearly increasing at rate of 100 V/μs.

mode with decrease in the initial radius of 4.5 mm due to developing instabilities under repeated action on the workpiece. However, for our version of instability excitation, condition (6) is certainly satisfied, since in this version it is necessary to maintain the stability of the conductor as a whole with respect to bending instability (3).

For a more in-depth analysis of the processes under consideration, it is advisable to evaluate what additional factors may influence the development of MHD instability, as well as to evaluate the dynamics of the process of formation and separation of droplets. This issue is considered qualitatively by numerical simulation in the Comsol Multiphysics environment of the pulsed current flow through cylindrical conductor, which material partially of in full is in a liquid state, when specifying an external effect in the form of a linearly increasing voltage on the conductor.

In the electrical part of the problem the conduction currents were calculated when external voltage was applied, in which the following equations were considered: law of current continuity $\nabla \mathbf{J}_{ec} = \nabla(\mathbf{J}_{\sigma,ec} + \mathbf{J}_{e,ec}) = 0$, where $\mathbf{J}_{ec}$, $\mathbf{J}_{\sigma,ec}$, $\mathbf{J}_{e,ec}$ total current density, conductivity and external influence; Ohm's law $\mathbf{J}_{\sigma,ec} = \sigma \mathbf{E}_{ec}$; and the connection between the intensity and the potential of the electric field: $\mathbf{E}_{ec} = -\nabla V$. The electrical problem is reduced to one equation regarding the electric potential:

$$\nabla(\sigma \nabla V + J_{e,ec}) = 0$$

and is solved in the AC/DC/Electric current module of Comsol Mltiphysics environment.

After solving this equation, it is possible to determine all the parameters of the electric field, including the distribution of conduction current density $\mathbf{J}_{\sigma,ec} = -\sigma \nabla V$ under the influence of external voltage, which is specified in the form of external influence $\mathbf{J}_{e,mf} = \mathbf{J}_{\sigma,ec}$ in the magnetic part of the problem.

In the magnetic part of the problem a system of magnetic field equations was considered, consisting of the total current law: $\nabla \times \mathbf{H} = \mathbf{J}_{mf} = \mathbf{J}_{\sigma,mf} + \mathbf{J}_{e,mf}$, where $\mathbf{H}$ — magnetic field strength vector, $\mathbf{J}_{\sigma,mf}$ $\mathbf{J}_{e,mf}$ — densities of conduction

current and external influence; Ohm's law: $\mathbf{J}_{\sigma,mf} = \sigma \mathbf{E}_{mf}$, σ — electrical conductivity, $\mathbf{E}_{mf}$ — electric field strength vector; law of electromagnetic induction: $\nabla \times \mathbf{E}_{mf} = -\frac{\partial \mathbf{B}}{\partial t}$, where $\mathbf{B}$ — magnetic field induction vector; and the connection of induction with magnetic potential $\mathbf{B} = \nabla \times \mathbf{A}$, consistent with Gauss's law for the magnetic field: $\nabla \cdot \mathbf{B} = 0$. The listed equations are reduced to one equation of the relative vector magnetic potential $\mathbf{A}$:

$$\Delta \mathbf{A} - \sigma \mu_{mf} \frac{\partial \mathbf{A}}{\partial t} = \mu_{mf} \mathbf{J}_{e,mf}$$

and are solved in the AC/DC/Magnetic fields module of Comsol Multiphysics environment. After solving this equation, you can determine all the parameters of the magnetic field, including the density of induced currents $\mathbf{J}_{\sigma,mf} = -\sigma \frac{\partial \mathbf{A}}{\partial t}$, which returns as an external influence to the electrical part of the problem $\mathbf{J}_{e,ec} = \mathbf{J}_{\sigma,mf}$ and the Lorentz force according to the following expression: $\mathbf{f}_L = \mathbf{j} \times \mathbf{B}$, which was specified as an external volume force acting on the liquid.

In the hydrodynamic part of the problem, the Navier–Stokes equation was solved for the laminar flow of an incompressible ($\nabla \cdot \mathbf{u} = 0$) Newtonian liquid:

$$\rho \frac{\partial \mathbf{u}}{\partial t} + \rho(\mathbf{u} \cdot \nabla)\mathbf{u} = -\nabla p + \mu_{hd} \Delta \mathbf{u} + \mathbf{f}_L$$

in the Fluid Flow/Laminar Flow module using Level Set module for modeling two-phase (liquid–gas) flow and the Two-phase Flow, Level set multiphysics interface connecting the two named modules between themselves. Depending on the change in the phase of the medium (liquid or gas), the following properties of the computational domain changed: density ρ, coefficient of dynamic viscosity μ_{hd} and electrical conductivity σ, i.e. when the liquid/gas interface moved/changed, the properties of the computational domains also moved/changed.

A problem was solved that was typical for systems associated with the release of high-density energy in conductor: current-carrying elements of cone type are mated with cylindrical conductor, while the electromagnetic problem and the hydrodynamic flow of the conducting fluid under the action of Lorentz forces are considered together, as described above when applying a linearly increasing voltage to the conductor at voltage rate of 100 V/μs. The modeling results for the case of thin, straightened outer layer of conductive material are shown in Fig. 7. It is clearly visible that in the interface zone between the conductor and the current supply, there is an increase in the Lorentz forces acting on the conductive material, which is associated with local increase in the current density in this zone. As the current flows, a portion of the material moves away from the field (towards the axis of the conductor) and the disturbance wave is developed, which leads to the generation of instabilities.

Regardless of the initial state of the conductor (completely or partially melted) in the initial phase of the process, the distribution of Lorentz forces leads to the same type scenario of instability development. It is obvious that the wavelength of the initial perturbation and the dependence of the growth rate of its amplitude depend on the interface angle, but the analysis of these relations is beyond the scope of this paper, and will be considered further.

Also note that the modeling did not take into account the change in conductivity as a result of heating. However, in accordance with numerous studies on the nonlinear diffusion of the magnetic field into conductor, one should expect a higher contrast in the distribution of Lorentz forces already in the initial loading phase, when the action integral did not reach value critical for the material, and the speed of transmission of these perturbations is close to the speed of sound in the medium. It can be expected that the structure configuration will depend not only on the homogeneity of the density distribution of the conductor and the quality of its surface treatment, but also is determined by the ratio of the wavelength generated by the inhomogeneous distribution of current (Lorentz forces) in the transition zone and the rate of current rise.

Comparing these calculations with the experimental results, we see that on copper conductors (Figs. 2 and 3) in the area where the conical transition interfaces the cylindrical part of the conductor, the perturbations are actually visible, approximately corresponding to those shown in the calculated graph in Fig. 7. On the duralumin sample (Fig. 4) these perturbations are expressed quite clearly. Stainless steel samples under the experimental conditions demonstrate less sensitivity to this factor. This may be due to a less pronounced surface effect than that of well-conducting conductors and, as a consequence, a less contrasting distribution of Lorentz forces in the contact zone; inertial effects due to the higher density of the material; uneven temperature distribution along the length of the conductor, due to the low thermal conductivity of steel, and the low duty cycle of the acting pulses, which is insufficient to establish thermodynamic equilibrium of the conductor between pulses. Studying the influence of the uneven distribution of Lorentz forces in the current supply zone on the formation of instabilities during MHD flow of liquid layers seems to be a separate problem, and is beyond the scope of this work.

To qualitatively evaluate the dynamics of the process of formation and separation of droplets on the surface of copper cylinder with diameter of 1.3 mm, an artificial initial perturbation was formed in the form of a sinusoid with amplitude of 0.1 mm, and the process of instabilities development was simulated for the case of completely liquid cylinder and a cylinder with a solid core of 1.2 mm, simulating the unmelted part of the conductor, when applying the same voltage linearly increasing at rate of 1 V/μs. The calculation results are presented in Fig. 8.

It can be seen that partial melting of the conductor leads to a decrease in the volume of droplets formed compared to the completely melted conductor. Simulation of the process of instabilities development shows that the violation

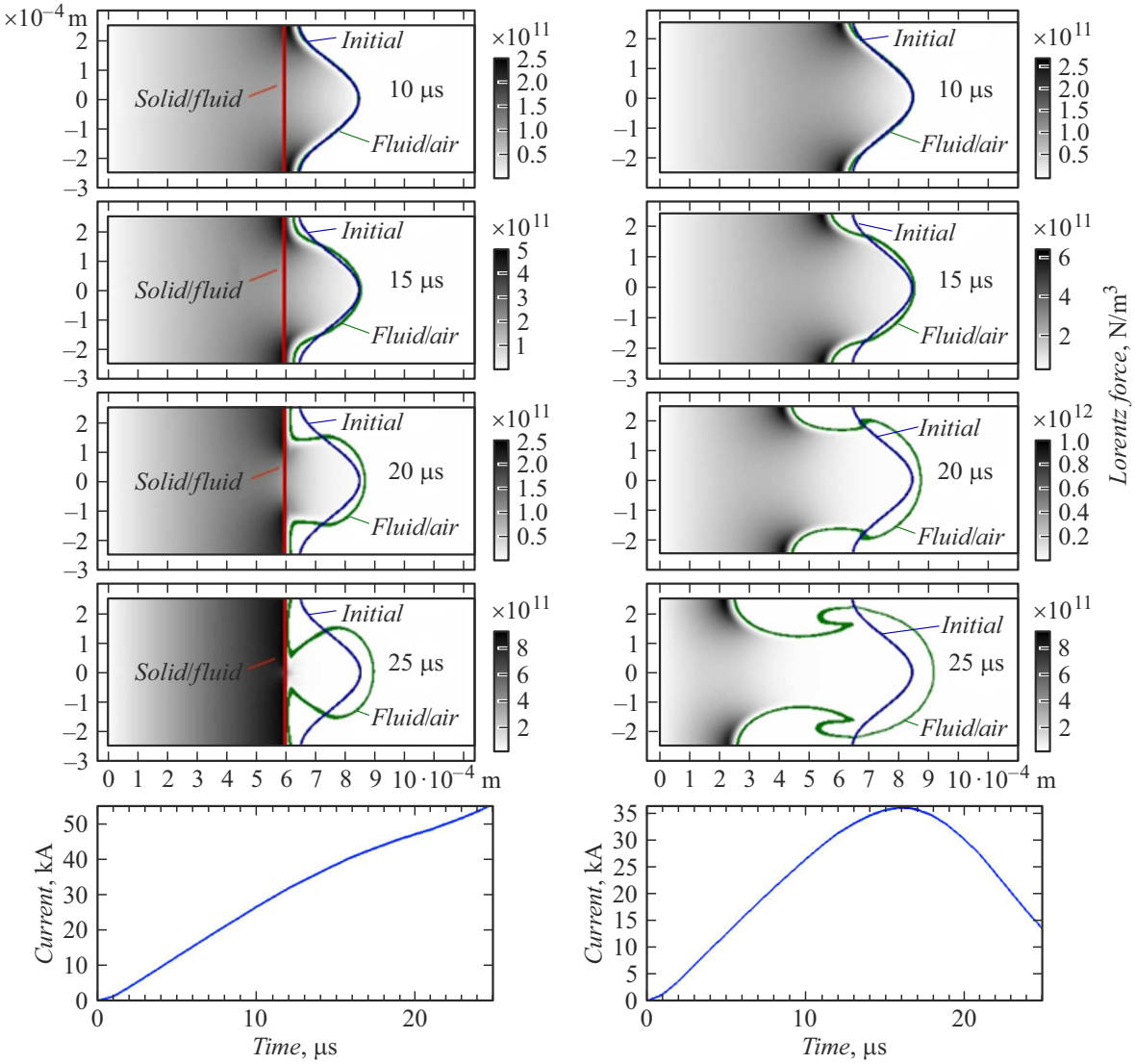

Figure 8. Development of the initial perturbation on the surface of conductor with solid core (left) and completely liquid core (right), and the corresponding graphs of current vs. time when applying voltage linearly increasing at rate of 1 V/ μs .

of homogeneity in the distribution of Lorentz forces acting at the crest and trough of the wave is responsible for their development. As expected, in accordance with [18] the current density at the wave crest is significantly less than in the wave trough, and the corresponding Lorentz forces, the distribution of which is shown in Fig. 8, lead to increase in the wave amplitude mainly due to material movement deep into the conductor. When a solid core is reached, the situation changes. The material from the straightened layer is pushed into the droplet zone, the dimensions of which are determined by the thickness of the molten layer and surface tension forces. The instability development in fully straightened conductor in the first moments occurs according to the same scenario; later, as the depth of the cavity increases, the current density in this zone increases, leading to increase in Lorentz forces directed deep into the conductor. In this case, a positive feedback effect is observed: the deeper the cavity is, the greater the current density is and, accordingly, the value of the Lorentz forces, under the influence of which the growth rate of the cavity depth increases. Due to increase in the depth of the cavity, the resistance of the conductor increases, which leads to decrease in the current flow. From comparison of the graphs in Fig. 8, it is clear that when the same linearly increasing voltage is applied in the case of completely molten conductor, its diameter becomes smaller than the diameter of partially molten conductor, which leads to a greater decrease in current.

Conclusion

Analysis of the modes of interaction of cylindrical conductor with flowing current sufficient for complete or partial melting of the material demonstrates not only

the multifactorial nature of the process of formation and development of instabilities, but also the possibility of predicting their development to form a given format of destruction.

The possibility of implementing the skin mode of conductor dispersion due to the instability development with wavelength close to the calculated one was experimentally demonstrated. The experimental results obtained are in good agreement with known theoretical estimates and the qualitative scenario of the dynamics of this process from the results of numerical simulation.

Analysis of the results of numerical simulation of MHD instabilities development at qualitative level demonstrated the relationship between the thickness of the molten metal and the size of the droplets, and revealed the influence of inhomogeneity in the distribution of Lorentz forces on the generation and development of MHD instabilities, and made it possible to identify additional factors that can have a significant impact on the considered process of MHD instability development, on the formation and separation of liquid metal droplets.

A skin explosion can be carried out in two ways: with complete layer-by-layer destruction of the conductor and with partial destruction of the surface layer of the conductor only. In the second case, you can save and study the central part of the conductor.

Using refractory steel as an example, the possibility of dispersing the surface layer of samples and forming microgranules with predictable sizes is shown.

Acknowledgments

The study results were obtained using the computing resources of the supercomputing center of Peter the Great St. Petersburg Polytechnic University.

Conflict of interest

The authors declare that they have no conflict of interest.

References

[1] V.I. Oreshkin, R.B. Baksht. IEEE Tr. Plasma Sci., **48** (5), 1214 (2020). DOI: 10.1109/TPS.2020.2985100
[2] N.V. Volkov, E.L. Fen'ko, A.E. Mayer, A.P. Yalovets, V.S. Sedoi. Tech. Phys., **55** (4), 509 (2010).
[3] V. Sorokin. Additivnye tekhnologii, 3, 21 (2022). (in Russian)
[4] V.S. Klimov, D.A. Karyagin, P.A. Erokhin. Tekhnologiya legkikh splavov, 3, 49 (2022).(in Russian).
[5] G.S. Garibov. Tekhnologiya legkikh splavov, 2, 38 (2021). (in Russian).
[6] K.B. Abramova, N.A. Zlatin, B.P. Peregud. ZhETF, **69** (6), 2007 (1975). (in Russian).
[7] M.L. Lev, B.P. Peregud, Z.V. Fedichkina. ZhTF, **46** (1), 125 (1976) (in Russian).
[8] S.D. Samuilov, A.A. Semenov. Magnitnaya gidrodinamika, 3, 4 (1987). (in Russian)
[9] S.D. Samujlov, A.A. Semenov. ZhTF, **62** (8), 38 (1992). (in Russian)
[10] K.B. Abramova, B.P. Peregud, S.D. Samuilov, A.A. Semenov. Nauchno-tekhnicheskie dostizheniya, 6, 17 (1988). (in Russian)
[11] S.D. Samuilov. *Proc. of the 15th International School-Conference on „New materials — Materials of Innovative Energy: Development, Characterization Methods and Application"* (Moscow, Russia, 2017), p. 524. DOI: 10.18502/kms.v4i1.2214
[12] S.D. Samujlov. Tekhnologiya metallov, 1, 6 (2018). (in Russian)
[13] G.A. Shvetsov, A.G. Anisimov, A.D. Matrosov. IEEE Tr. Magn. **39** (1), 82 (2003).
[14] E.I. Starovojtenko. Tekhnologiya legkikh splavov, 1, 4 (2022). (in Russian).
[15] S.B. Batuev, Sh.M. Shejkhaliev, S.I. Popel, V.A. Kozmin. AS. 1121101 (SSSR). B.I., 40 (1984). (in Russian)
[16] S.A. Chaikovsky, V.I. Oreshkin, I.M. Datsko, N.A. Labetskaya, D.V. Rybka, N.A. Ratakhin. Phys. Plasmas, **22** (11), 112704 (2015). DOI: 10.1063/1.4935401
[17] V.I. Oreshkin, S.A. Chaikovsky, I.M. Datsko, N.A. Labetskaya, G.A. Mesyats, E.V. Oreshkin, N.A. Ratakhin, D.V. Rybka. Phys. Plasmas, **23** (12), 122107 (2016). DOI: 10.1063/1.4971443
[18] S.I. Krivosheev, S.G. Magazinov, G.A. Shneerson. Pisma v ZhTF, **45** (3), 41 (2019) (in Russian). DOI: 10.21883 (in Russian)

Translated by I.Mazurov